Global Change Biology (2008) **14**, 768–781, doi: 10.1111/j.1365-2486.2007.01526.x

# Dry nitrogen deposition estimates over a forest experiencing free air $CO_2$ enrichment

JED P. SPARKS*, JOHN WALKER†, ANDREW TURNIPSEED‡ and ALEX GUENTHER‡
*Department of Ecology and Evolutionary Biology, Cornell University, Ithaca, NY 14853, USA, †National Risk Management Research Laboratory, United States Environmental Protection Agency, Research Triangle Park, NC 27711, USA, ‡National Center for Atmospheric Research, Atmospheric Chemistry Division, Boulder, CO 80307, USA

**Abstract**

**The quantification of atmospheric additions of nitrogen (N) to an ecosystem is often desirable, but difficult for many locations including many ecological manipulation experiments. Ideal methodologies for the complete and chemically speciated quantification of dry N deposition (e.g. tunable diode laser absorption spectrometer, thermal-dissociation laser-induced fluorescence) are expensive, technologically challenging to maintain, and rarely colocated with important global change manipulation experiments. Here we present an alternative method for obtaining an approximation of total N deposition using short-term eddy flux and concentration measurements, annual regional concentration estimates, and modeling for the Duke Experimental Forest. The motivation for generating estimates for this location was to inform the long-term elevated $CO_2$ experiment conducted at Duke Forest. We estimated the total annual atmospheric N deposition to the forest to be 13.7 kg N ha$^{-1}$. Of this total, ~58% was in dry-deposited forms. Surprisingly, and contrary to some previous predictions, nitric acid ($HNO_3$) was not the dominant portion of the total dry-deposited N, implying strongly that other forms of gaseous N like organic peroxy and alkyl nitrate compounds are a significant portion of the total flux. Furthermore, this study sheds light on the completeness of the estimates derived from Clean Air Status and Trends Network (CASTNet) and other dry deposition networks. CASTNet does not measure organic forms of dry deposition. In fact, CASTNet only quantifies $HNO_3$ in the gas phase and may significantly underestimate total N deposition in many environments.**

*Keywords:* ammonia, nitric acid, nitrogen deposition, peroxynitrate

*Received 30 October 2006; revised version received 15 July 2007 and accepted 18 August 2007*

## Introduction

The primary inputs of available nitrogen (N) to ecosystems (excluding the direct addition of fertilizers) are biological fixation by organisms, N-containing compounds in precipitation, and the direct removal of gases or particles from the atmosphere. Biological fixation and the N contained in precipitation (i.e. wet deposition) are routinely monitored and estimated at many ecological research sites including those aimed at understanding the influence of global change. However, the deposition of gases and particulates (i.e. dry deposition) is rarely reasonably constrained at such sites. The importance of this 'dry' depositional pathway has been recognized for over 50 years (Meetham, 1950), but technological constraints have made direct measurements challenging. Dry deposition is an important pathway for ammonia (Sutton *et al*., 1995), nitrogen dioxide (Duyzer *et al*., 1995; Duyzer *et al*., 2004), and nitric acid ($HNO_3$) (Dollard *et al*., 1987). Therefore, quantifying the dry deposition of these compounds is often imperative to close the N budget of a particular ecosystem.

A multitude of studies are currently underway investigating the influences of global change and, in most, the quantification of dry-deposited N is imperative for understanding ecosystem function. Therefore, the motivation for constraining dry N deposition estimates is high in the ecological community. In recent years, new technologies have been applied to directly and continuously measure the dry deposition of N. For example, Horii *et al*. (2005) and Farmer *et al*. (2006) have reported total reactive N ($NO_y$) and $HNO_3$ flux estimates using

Correspondence: Jed P. Sparks, e-mail: jps66@cornell.edu

tunable diode laser absorption spectrometery and thermal-dissociation laser-induced fluorescence to pine-forest ecosystems in California. These methods show great promise. However, they are expensive, technologically challenging to maintain, and, because of these constraints, are unlikely to be colocated with many important global change manipulation experiments. Here, we present an alternative method for obtaining an approximation of total N deposition using short-term eddy flux and concentration measurements, annual regional concentration estimates, and modeling. We use the Duke Experimental Forest as a case study and as an exemplar global change experiment site.

There are currently several large-scale experiments examining the influence of elevated $CO_2$ on terrestrial ecosystem function [e.g. free air $CO_2$ enrichment (FACE) experiments conducted at Duke Forest, on the Nevada Test Site, Rhinelander, and Illinois]. Most investigations to date show an increase in woody biomass under elevated atmospheric $CO_2$ (e.g. Bazzaz & Miao, 1993; Curtis & Wang, 1998; Zak *et al*., 2000; Hamilton *et al*., 2002) and a potential role of woody ecosystems in sequestering carbon in the future (Schimel *et al*., 2001). However, the growth response to elevated $CO_2$ in woody plants appears, in many systems, to be constrained by the availability of soil nutrients, most notably N (Pan *et al*., 1998; Luo *et al*., 1999; Zak *et al*., 2000; Oren *et al*., 2001). Although there is some debate as to what ecosystems will respond to added N (e.g. Ollinger *et al*., 2002), these two observations underscore the need to estimate both endogenous cycling of N within the ecosystem and all of the exogenous inputs and losses if we are to predict future function. The most challenging of these estimates is the dry deposition of gases and particles. Measurement methodologies are expensive and technologically intensive. A method that could be broadly applied at a reasonable price would be beneficial to global change research. To that end, the work reported here examines the atmospheric input of gaseous and particulate N to a forested system using a combination of empirical measurements and modeling to generate a constrained estimate of dry N deposition to Duke Forest, an important ecological global change research site currently receiving elevated levels of $CO_2$.

The measurements we present here were made as part of the Chemical Emission, Loss, Transformation and Interactions within Canopies (CELTIC) study conducted at the Duke Forest FACE site during the summer of 2003. The overarching goal of CELTIC was to develop a quantitative understanding of the processes controlling the exchange of gas and aerosol carbon and N between the atmosphere and vegetated canopies. The CELTIC study addressed emission and deposition of volatile organic carbon and N, as well as the formation and deposition of secondary organic and inorganic aerosol, through measurements and modeling from leaf to canopy scales. The work presented here focuses primarily on the N flux measurements made as part of the CELTIC experiment.

Estimates of dry deposition of reactive N to individual plants or entire ecosystems have been made using dynamic and open-topped chambers (Gessler *et al*., 2000; Sparks *et al*., 2001) and by measuring precipitation throughfall after it passes through the plant canopy (Lovett *et al*., 2000). However, these methods preclude deposition to nonplant surfaces, chemical transformations within or above the canopy, and attempts to scale chamber measurements to whole-system fluxes are associated with a high degree of uncertainty (Hanson *et al*., 1989). The best regional estimates of dry N deposition come from the EPA-sponsored Clean Air Status and Trends Network (CASTNet) sites. However, CASTNet sites only measure a subset of dry-deposited N (particulate $NO_3^-$ and $NH_4^+$ and gas-phase $HNO_3$) and do not quantify several important species of gaseous N (e.g. $NH_3$, and major components of total $NO_y$ including $NO_2$, $N_2O_5$, HONO, PANs, and alkyl nitrates). In addition, CASTNet sites are relatively rare and are often not colocated near global change experiments.

Micrometeorological techniques, including eddy covariance, resistance analogies, and Bowen ratio methods, have been used to estimate total dry deposition (e.g. Meyers *et al*., 1996; Munger *et al*., 1996; de Miguel & Bilbao, 1999; Nemitz *et al*., 2001). However, these studies often focus only on part of the total dry deposition based on a molecule of interest and do not quantify the entire flux and they are rarely conducted at research sites examining global change.

Our goal with this work was to provide an estimate for total N deposition in the gas and particle phase to an experimental forest where $CO_2$ is artificially elevated. This estimate is extremely useful in the context of evaluating the N input and, hence, N dynamics of this system. Although specific to this location to make it relevant to an important global change manipulation experiment, the results and techniques presented are generalizable to any forested system. Secondarily, we were interested in partitioning the potential inputs by chemical species and quantifying the seasonal variation in dry N input to the system. Our approach was to use direct flux measurements of $NO_y$ and concentration measurements of $HNO_3$, $NH_3$, particulate $NH_4^+$, and $NO_3^-$ in conjunction with long-term measurements at nearby North Carolina Division of Air Quality (NC DAQ, 2005) and CASTNet (2005) sites to infer an annual input of N to this system from the atmosphere.

 

**Table 1** Sites from which data was used in the present study

| Site name | Type | Distance*/direction from Duke Forest | Description | Species measured |
|---|---|---|---|---|
| Candor | CASTNet | 95/SW | Rural/forest | $HNO_3$, $NO_3^-$, $NH_4^+$ |
| Clinton | NC DAQ | 125/SE | Rural/agricultural | $NO_y$ |
| Kinston | NC DAQ | 155/SE | Suburban | $NO_y$ |
| Charlotte | NC DAQ | 180/SW | Urban | $NO_y$ |
| Winston-Salem | NC DAQ | 120/W | Urban | $NO_y$ |
| Morehead City | UNC IMS | 250/SE | Urban/coastal | $NH_3$ |

*Distance in kilometers.
CASTNet, Clean Air Status and Trends Network; NC DAQ, North Carolina Division of Air Quality.

## Materials and methods

### *Site description*

Flux measurements were conducted at the Duke Forest FACE site between July 11 and 25, 2003 [day of year (DOY) 191–206] within one of the control plots (i.e. no $CO_2$ enhancement). The site has been described in depth previously, both in terms of its physical and biological properties, and its suitability for measurement of ecosystem level fluxes by eddy covariance (Katul & Albertson, 1999). Therefore, we will present only a brief description here. The forest consists of a Loblolly pine (*Pinus taeda*) plantation with an average canopy height ($h_c$) of 17 m and an LAI of $3.5\,m^2\,m^{-2}$ (Katul & Albertson, 1999). The understory consists of a mixture of hardwood species dominated by sweetgum (*Liquidambar styraciflua*). Sweetgum individuals were typically $\leq$10 m in height, although some individual trees extended into the upper canopy. Vegetation was homogeneous in the primary wind direction (southwest) for $\sim$1 km.

### *Long-term data sites*

Data from four NC DAQ long-term air quality stations and one CASTNet station were used to scale depositional data for Duke forest. Two of the NC DAQ sites are in urban areas and two are located in more rural settings. In addition, $NH_3$ data from a coastal site operated by the UNC Institute of Marine Sciences were also used to help quantify gaseous $NH_3$ fluxes. Table 1 gives an overview of the sites and distances from the primary Duke Forest field site where flux measurements were made.

### *Eddy covariance fluxes of $NO_y$*

A detailed description of the $NO_y$ flux measurements and data analysis has been given in Turnipseed *et al*. (2006) and only a brief description will be presented here. Flux measurements were made at a height of 26 m. Three-dimensional wind velocities ($u$, $v$, $w$) were measured at 10 Hz by a sonic anemometer (ATI-K, Advanced Technologies Inc., Boulder, CO, USA). $NO_y$ fluxes were measured similar to the method described by Munger *et al*. (1996). Sample air at 2000 sccm was drawn into a heated catalytic converter containing a 60 cm piece of $\frac{1}{4}''$ gold tube at 295 °C. A small flow of $H_2$ (25 sccm) was added just before the heated region to help reduce oxidized N species to NO (Fahey *et al*., 1985). The flow was then passed to an NO analyzer (Ecophysics CLD 770 AL ppt, Duernten, Switzerland). The CLD 770 AL ppt generates a excess source of ozone, reacts it with the sample flow, and detects light from the chemiluminescent reaction between NO and $O_3$:

$$NO + O_3 \rightarrow NO_2 + O_2 + h\nu. \quad (1)$$

Light emission was detected by a red-sensitive photomultiplier tube and the subsequent current pulses were amplified and counted directly by a PC and recorded at 10 Hz. The analyzer avoids interferences using a prereaction chamber where $O_3$ is used to consume NO before entering the reaction chamber. Because the rate of reaction with NO is very fast and the reaction with most interference compounds is relatively slower, two sequential runs (the first utilizing the prereaction cell and second going directly to the sample cell without prereaction) allows for the quantification of NO independent of interferences. The analyzer was calibrated daily via standard addition by injecting a small flow (1–10 sccm) of NO standard (1.9 ppm $NO/N_2$) at the inlet. These tests (conducted upon each calibration) also indicated an adequately fast response ($\tau < 0.5$ s, 1/e). The conversion efficiencies and losses of $NO_y$ within our system are discussed more fully in Turnipseed *et al*. (2006). Simply stated, it is likely that there was some loss of $HNO_3$ within the initial inlet, although the exact amount of loss under the experimental conditions was difficult to quantify. Therefore, it is possible that our $NO_y$ fluxes may be underestimated by up to $\sim$35%.

Before calculation of fluxes, wind coordinates were rotated such that $\bar{v} = \bar{w} = 0$ (Kaimal & Finnigan, 1994), and scalar time series were despiked, linearly detrended, and shifted in time relative to $w$ to account for lags induced by the inlet line. These lags were determined via cross correlation between the vertical wind velocity, $w$, and $NO_y$. Fluxes were then calculated from the covariance between vertical wind velocity ($w$) and total $NO_y$ density.

### *Concentrations and fluxes of $NH_3$, $HNO_3$, $NH_4^+$, and $NO_3^-$*

Gas-phase $NH_3$ and $HNO_3$, and particulate $NH_4^+$ and $NO_3^-$ were measured by annular denuder/filter pack system (ADS; US EPA, 1997; Walker *et al*., 2004). Triplicate samples were collected over 12-h periods (06:00–18:00 hours day cycle; 18:00–06:00 hours night cycle). Measurements were taken at a height of 2 m above the forest floor from July 10 to 16 and at 22 m, just above the canopy, from July 16 to 24. Sample air was drawn via a pump through the ADS (URG Corporation, Chapel Hill, NC, USA) through the following components in series: an aluminum Teflon-coated cyclone (10 Lpm, $<2.5\,\mu m$ cutoff), two annular denuder tubes (30 mm OD $\times$ 242 mm length), a two-stage Teflon filter pack, and a third denuder tube. The Teflon filter pack contains a Teflon filter (47 mm diameter) followed by a nylon filter. The nylon filter and third denuder capture $HNO_3$ and $NH_3$, respectively, which are produced when $NH_4NO_3$ is lost by volatilization from the primary Teflon filter. Denuders and filters were extracted with 10 and 5 mL of deionized water, respectively, and analyzed by ion chromatography (Dionex Corporation, Sunnyvale, CA, USA). Measurement uncertainties, expressed as the median coefficient of variation from triplicate samples, were 24%, 11%, 11%, and 27% for $NH_3$, $NH_4^+$, $HNO_3$, and $NO_3^-$, respectively.

During CELTIC, the denuder/filterpack system was not deployed in a configuration that allowed for the direct determination of fluxes. This is primarily due to the difficulty in achieving acceptable precision at short sampling times required by traditional micrometeorological flux measurement techniques. We have, therefore, estimated fluxes of $NH_3$, $NH_4^+$, $HNO_3$, and $NO_3^-$ using a combination of measurements and modeling, which is a common approach when only routine chemical and meteorological data are available (Meyers *et al*., 1998; US EPA, 2004). Only chemical and meteorological measurements taken above the canopy were used to estimate dry deposition fluxes from the model simulation. For each chemical species, hourly deposition fluxes ($F$) were calculated by applying 12-h integrated air concentrations ($C$) to hourly deposition velocities ($V_d$) (i.e. $F = CV_d$).

Particulate $NO_3^-$ and $NH_4^+$ deposition velocities were estimated using a version of Slinn's (1982) model, modified to account for particle speciation and surface wetness (Ruijgrok *et al*., 1997). Deposition rates for $HNO_3$ and $NH_3$ were calculated using the classic resistance analogy (Hicks *et al*., 1987) in which the deposition velocity is viewed as the reciprocal of the sum of resistances to deposition due to turbulence ($R_a$, calculated via Garland, 1977), diffusion across the quasi-laminar sublayer of air surrounding the receptor elements ($R_b$, calculated via Meyers *et al*., 1989), and surface uptake processes that collectively determine the canopy resistance ($R_c$). For $HNO_3$, $R_c$ is a function of the dynamic stomatal resistance (Monteith & Unsworth, 1990) and static cuticular ($R_w$) and ground ($R_g$) resistances. Based on the approaches of Brook *et al*. (1999) and Meyers *et al*. (1998), $R_w$ and $R_g$ are both set to a value of $30\,s\,m^{-1}$.

Forests act as both sources and sinks of $NH_3$, depending on the ambient $NH_3$ concentration, leaf and soil N status, and other environmental factors (Duyzer *et al*., 1992; Wyers & Erisman, 1998; Pryor *et al*., 2001). For this reason, the bidirectional canopy-scale $NH_3$ flux was calculated using a canopy compensation point model developed by Sutton *et al*. (1998). This is similar to the resistance model used for $HNO_3$ except that it includes a stomatal compensation point and soil emission. The stomatal compensation point ($\mu g\,NH_3\,m^{-3}$) was calculated according to Nemitz *et al*. (2000) as a function of temperature and the leaf emission potential $\Gamma_s = [NH_4^+]/[H^+]$. In this study we used $\Gamma_s = 250$, which is well within the range of values reported for low N systems (Flechard & Fowler, 1998; Schjoerring *et al*., 1998; Milford *et al*., 2001). Finally, we specified a static soil emission flux of $5.0\,ng\,NH_3\,m^{-2}\,s^{-1}$ based on flux measurements from other unfertilized soils in North Carolina (Walker *et al*., 2002).

## Results and discussion

### *Concentration and flux measurements*

During the time period of the CELTIC experiment, $NO_y$ fluxes and concentrations were monitored over Duke Forest (Fig. 1). In general, $NO_y$ concentrations were highest in the early morning and late evening after 18:00 hours (averages $\sim$6.5–7.5 ppbv), likely due to a combination of local traffic patterns and lower boundary layer heights during these periods. Average daytime $NO_y$ fluxes tended to be between $-20$ and $-25\,ng\,N\,m^{-2}\,s^{-1}$ (Fig. 1b). In addition, $NO_y$ deposition reached a maximum at midmorning and was substantially lower

 

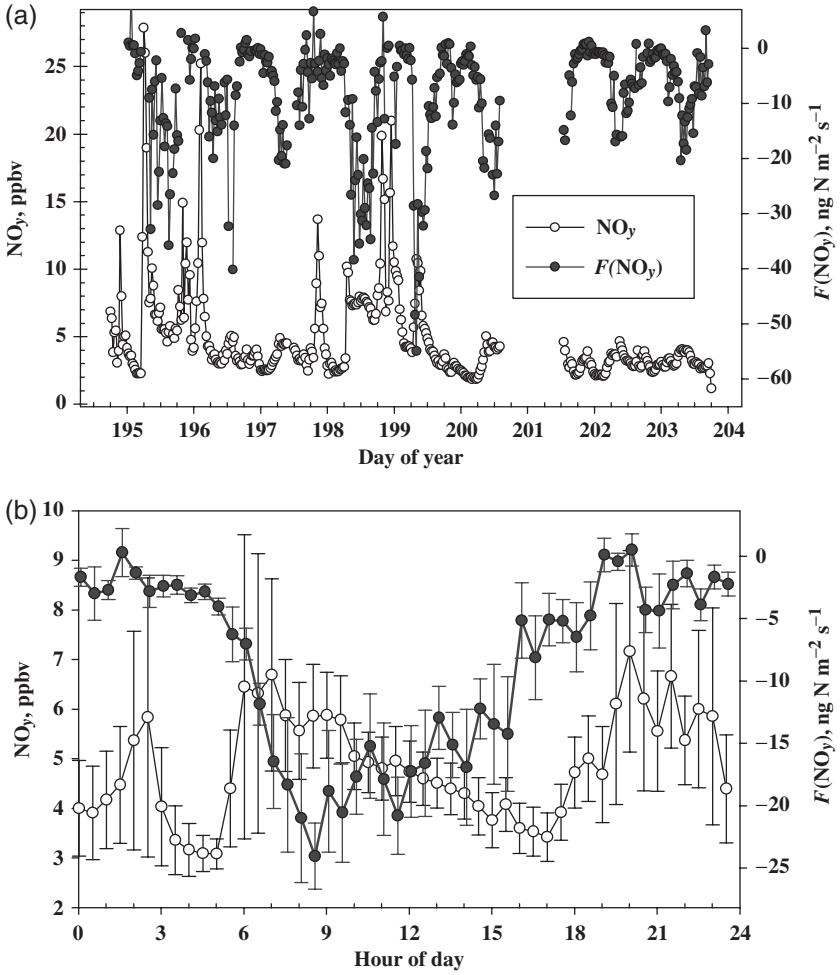


**Fig. 1** (a) $NO_y$ concentrations and fluxes measured during Chemical Emission, Loss, Transformation and Interactions within Canopies (CELTIC) study at the Duke Forest free air $CO_2$ enrichment (FACE) site. (b) Diurnal average $NO_y$ concentration and flux during CELTIC. Error bars are the standard error.

during the night-time hours due to decreased turbulent mixing. On average, about 0.75 mg N $m^{-2}$ was deposited daily. This is in reasonable agreement with the daily $NO_y$ flux estimates of 0.35–0.70 mg N $m^{-2}$ $day^{-1}$ reported by Munger *et al*. (1996) over a deciduous forest in the northeast United States.

Denuder/filterpack measurements above and below the canopy are summarized in Fig. 2a. Concentrations of $HNO_3$, $NO_3^-$, and $NH_4^+$ were higher above the canopy, suggesting a net sink for these compounds. This pattern was consistent for day and night periods, though individual chemical species exhibited diurnal variability (Fig. 2b). Photochemical cycling of $NO_x$ from local traffic resulted in higher concentrations of $HNO_3$ and $NO_3^-$ during daytime hours. Concentrations of $NH_4^+$ were also higher during the day, consistent with higher daytime concentrations of $SO_4^{-2}$ and $NO_3^-$.

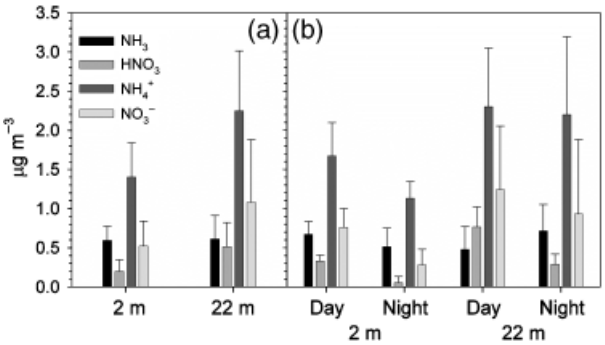


**Fig. 2** Average concentrations of $NH_3$, $HNO_3$, $NH_4^+$, and $NO_3^-$ measured above (22 m) and below (2 m) the forest canopy (a) during the entire study period and (b) by day (06:00–18:00 hours) and night (18:00–06:00 hours) periods. Error bars represent the standard deviation of the mean.

 

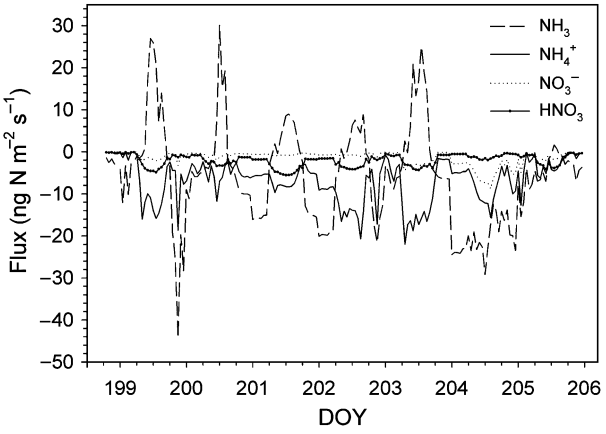


**Fig. 3** Modeled fluxes of $NH_3$, $HNO_3$, $NH_4^+$, and $NO_3^-$ during Chemical Emission, Loss, Transformation and Interactions within Canopies (CELTIC) study.

Modeled $HNO_3$, $NO_3^-$, and $NH_4^+$ fluxes (Fig. 3) are consistent with the observed concentration gradients, and correspond to net deposition fluxes of 2.05, 1.43, and $6.85\,ng\,N\,m^{-2}\,s^{-1}$, respectively, over the entire study period. Modeled deposition fluxes of these species are highest during the late morning and early afternoon, reflecting the combination of higher concentrations and more effective turbulent mixing during daytime hours.

As described above, $HNO_3$ deposition was estimated independently of $NO_y$ during the CELTIC experiment. Gas phase $HNO_3$ deposition is a subset of the total $NO_y$ flux and comparisons of the two measurements can be used to estimate the proportion of the total $NO_y$ flux that is gaseous $HNO_3$. During the CELTIC measurement period, the weekly sum of deposited $NO_y$ was $5.25\,mg\,N\,m^{-2}$ compared with $1.24\,mg\,N\,m^{-2}$ of $HNO_3$ (estimated from direct concentration measurements and resistance modeling). Therefore, $HNO_3$ constituted $\sim 24\%$ of the $NO_y$ flux, which agrees with other recent studies (Sparks *et al*., 2003; Turnipseed *et al*., 2006) suggesting organic nitrate and peroxynitrates may represent a large fraction of the total dry-deposited oxidized N and contradicting the common notion that $HNO_3$ dominates total N deposition at most sites (Williams *et al*., 1997).

Ammonia concentrations tended to be similar above and below the canopy. This pattern suggests a small net flux or the presence of an $NH_3$ source in the lower canopy, most likely soil and decaying organic matter. Emissions from these sources are expected to increase with temperature when soil mineralization and litter decomposition rates are highest. The temperature dependence of these sources, in combination with the diurnal cycle of dew at the forest floor, most likely explains the higher daytime concentrations of $NH_3$ observed below the canopy (Fig. 2b). In contrast, the observed higher concentrations of $NH_3$ above the canopy at night may reflect the influence of boundary layer depth (Fig. 2b). In both cases, however, the differences in average day and night-time concentrations are small. Over the entire study period, the canopy compensation point model yielded a net downward flux of $5.76\,ng\,NH_3\text{-}N\,m^{-2}\,s^{-1}$ in spite of a consistent pattern of emission during daytime hours. During periods of emission, the ambient concentration of $NH_3$ was below the predicted canopy compensation point. This diurnal pattern of bidirectional exchange is consistent with the relatively low concentrations of $NH_3$ observed during the experiment ($0.23\text{–}1.15\,\mu g\,m^{-3}$), which were always close to the predicted canopy compensation point ($0.01\text{–}1.6\,\mu g\,m^{-3}$).

### *Scaling to annual estimates*

Because our measurements covered a relatively short period of time ($\sim$15 days), annual deposition was estimated using representative data from the nearest long-term measurement sites. Given the significant uncertainties inherent in such an exercise, we present deposition calculations for individual chemical species or total $NO_y$ using multiple approaches (scenarios) in an effort to provide a range of estimates.

### *Annual $NO_y$ fluxes*

Figure 4a shows $NO_y$ concentrations measured at several sites across North Carolina. Although there is considerable day-to-day variability between sites, trends on longer time scales (many days to weeks) are well correlated. This suggests that regional scale meteorology plays a large role in governing mean trace gas concentrations across North Carolina and supports our contention that concentrations measured at these various sites over the annual time scale will be relevant to the Duke site.

Figure 4b shows $NO_y$ concentrations measured at rural and urban NC DAQ measurement sites and measurements made at Duke Forest during CELTIC. Some correlations among sites can be seen and our measurements tend to fall within the range observed at the rural NC DAQ sites (12-h running averages correlated to CELTIC measurements; $r^2 = 0.56$). This is illustrated in Fig. 4c showing the average diel profile for $NO_y$ concentration for the month of July at the various NC DAQ sites and our measured data at Duke Forest (between DOY 194 and 205, July 13–24). Again, the Duke Forest measurements consistently overlap with the rural site estimates.

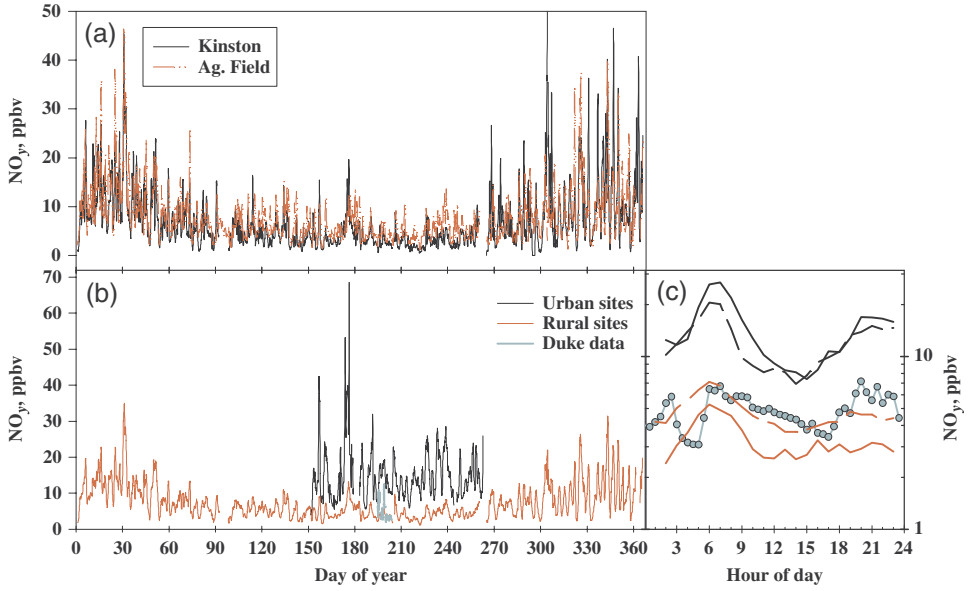


**Fig. 4** (a) Time series of $NO_y$ measurements from the two rural NC DAQ monitoring sites for 2003. (b) Average $NO_y$ concentrations from the two rural NC DAQ sites relative to the average $NO_y$ measured at the two urban NC DAQ sites for 2003. Our measurements from the Duke site are included. (c) Average diurnal profile of $NO_y$ concentrations from the four NC DAQ sites for the month of July 2003, and that measured at Duke Forest.

These diel profiles point out another important aspect of congruency between sites. Even though larger scale meteorology appears to govern the mean $NO_y$ concentration, all sites, regardless of whether they were situated in urban or rural areas, tended to show similar diel patterns (Fig. 2c). The observed concentration peaks in the morning and evening are consistent with low boundary layer heights and significant local $NO_x$ emission (e.g. traffic patterns).

The general consistency between $NO_y$ concentration measurements from the rural long-term sites and the Duke Forest measurements allowed us to scale our limited dataset to an annual deposition estimate. The scaling strategy was to apply the correlation between the real-time measurements made concurrently in the two locations to predict concentrations at Duke Forest during other times of the year.

The primary uncertainty associated with this extrapolation strategy is that $NO_y$ consists of multiple chemical species that have different seasonal cycles, deposition characteristics, and sources, and the $NO_y$ deposition is the net flux of their sum. The majority of $NO_y$ in moderately polluted environments such as North Carolina consists of $NO_x$ ($NO + NO_2$, 40–80%, Williams *et al*., 1998). NO is emitted from soils with essentially no uptake by vegetation (Hereid & Monson, 2001). $NO_2$ is also produced by soils, but is primarily produced in urban and suburban areas by the burning of fossil fuels. $NO_2$ can be either emitted or taken up by vegetation depending upon the ambient concentration (Sparks *et al*., 2001). The remaining components of $NO_y$ consist of more oxidized forms of N such as organic nitrates, peroxynitrates, and $HNO_3$. It has been suggested that a majority of the dry N flux to most vegetated surfaces is due to $HNO_3$ vapor although it makes up only 2–10% of the total $NO_y$ composition (Williams *et al*., 1997). However, this study, other measurements made during CELTIC (Turnipseed *et al*., 2006), and other recent work (Sparks *et al*., 2003) suggest that peroxynitrates deposit more readily to vegetation than was once thought and can make a significant contribution to the total $NO_y$ flux. Given the potential variation in total dry N driven by the compositional differences of $NO_y$ outlined above, we have used four scenarios devised to encompass the possible range of $NO_y$-deposition values. These scenarios are described below and the annual sums are shown in Table 2. The results across the four scenarios represent an upper and lower bound on the potential annual dry deposition of N to Duke Forest.

Scenario (1) was based on the measurements at Duke Forest indicating that midday $NO_y$ fluxes show a linear relationship with concentration, giving a constant deposition velocity (slope) of $0.9\,cm\,s^{-1}$ ($R^2 = 0.69$, $N = 163$). This relationship does not hold for night-time data. At night when turbulent transport limited deposition, $V_d(NO_y)$ varied with turbulence (denoted by the friction velocity, $u^*$). Average $[NO_y]$ from the two rural sites was combined with friction velocity and solar radiation information from the Duke Forest AmeriFlux

**Table 2** Annual dry N deposition for individual chemical species to Duke Forest during 2003

| Scenario (see text for description) | $NO_y$ | $HNO_3$ | $NH_3$ | $NO_3^-$ | $NH_4^+$ |
|---|---|---|---|---|---|
| 1 – Constant flux | 5.40 | 1.56 | 2.07 | 0.043 | 0.41 |
| 2 – Constant flux II | 2.74 | 1.38 | 1.59 | 0.058 | 0.46 |
| 3 – Corrected flux ($HNO_3$ and $NO_3^-$) | 2.35 | 1.95 | −0.180 | 0.29 | 1.67 |
| 4 – Corrected flux (ratio) | 4.34 | 2.90 | 1.90 | na | na |
| **5** –Ammonia | na | na | 1.22 | na | na |

All measures are in kg N $ha^{-1}$. Scenario refers to the model used to generate each estimate. See the text for details.
CASTNet, Clean Air Status and Trends Network.

site to estimate the total flux of deposited N to the surface.

The shortcomings of scenario (1) are that it assumes that all species of $NO_y$ contribute equally to the deposition flux and/or the $NO_y$ composition remains the same regardless of season. Neither of these assumptions is likely to be valid. Photochemical conversion of $NO_x$ to more oxidized N species (e.g. $HNO_3$) occurs more readily during the summer (i.e. higher light levels and temperatures lead to more rapid photochemical conversion). However, because anthropogenic emissions of $NO_y$ (consisting mostly of $NO/NO_2$ from combustion) remain relatively constant throughout the year, a seasonal cycle in the $NO_y$ partitioning is typically observed with $NO_x$ constituting a higher fraction of $NO_y$ during winter periods. Furthermore, $NO_y$ concentrations are often higher at the surface during winter due to lower boundary layers (see Fig. 4a and b). These larger wintertime concentrations and the assumption of a constant year-long deposition velocity for $NO_y$ yields an overestimate of N deposition using this analysis, but may be viewed as an upper limit to total $NO_y$ deposition.

Scenario (2) builds on the observations presented by Munger *et al*. (1996). Their long-term measurements over Harvard Forest (a deciduous forest located in Massachusetts, USA) suggested similar fluxes of $NO_y$ (but not deposition velocity) regardless of season. Therefore, this scenario assumes the average diurnal flux measured during the July measurement period at Duke is applicable throughout the year (i.e. the distribution of chemical compounds within $NO_y$ is fixed throughout the year). This is obviously a simplification of the mechanism because it does not require any knowledge of annual trends in concentrations.

Scenarios (3) and (4) are based on the assumption that the $NO_y$ flux is dependent on the most highly oxidized fractions of $NO_y$ (i.e. $HNO_3$ and $NO_3^-$), which are most readily deposited. The sum of $NO_3^- + HNO_3$ from the nearest CASTNet site (Candor, NC, USA) was used to estimate this 'oxidized fraction.' Subsequently, hourly $NO_y$ concentrations from the rural and suburban NC DAQ sites were averaged by week and temporally aligned with the CASTNet measurements. Weekly $NO_y$ fluxes for scenario (3) were then determined by scaling the average weekly flux measured during CELTIC (5.25 mg N $m^{-2}$ $week^{-1}$) by the ratio of the highly oxidized fraction of $NO_y$, $(\{NO_3^- + HNO_3\}_i/\{NO_y\}_i$ where $i$ represents the week number relative to the fraction observed during week 28). Scenario (4) was generated in a similar fashion, except that the average weekly flux was scaled by the ratio of the total amount of $HNO_3 + NO_3^-$ for a given week relative to that on week 28, $(NO_3^- + HNO_3)_i/(NO_3^- + HNO_3)_{i=28}$. CELTIC $NO_y$ measurements spanned week 28 of 2003.

Annual $NO_y$ sums for all four scenarios are given in Table 2. As described above, scenario (1) likely leads to an upper limit of 5.4 kg N $ha^{-1}$ $yr^{-1}$. Conversely, scenario (2) will likely lead to a lower limit as it does not take into account both increased $NO_y$ (from rural NC DAQ stations) and $HNO_3$ (from CASTNet sites) concentrations during winter, which should lead to higher deposition rates. Scenario (3) may also be negatively biased as the highly oxidized fraction of $NO_y$ decreases in winter. Because scenario (4) is scaled directly to $HNO_3 + NO_3^-$ concentrations, it should provide the most reliable estimate of the seasonal changes in $NO_y$ flux and, thus, its result of 4.34 kg N $ha^{-1}$ $yr^{-1}$ is likely to be the most accurate estimate.

### *Annual $HNO_3$, $NO_3^-$, and $NH_4^+$ fluxes*

To estimate $HNO_3$ deposition independently from $NO_y$, we again utilized four scenarios to provide an upper and lower bound for $HNO_3$ deposition to Duke Forest. The first scenario takes the measured Candor CASTNet concentration as a proxy for Duke Forest and calculates $HNO_3$ fluxes using a resistance-based multilayer model (MLM; Meyers *et al*., 1998) to produce weekly estimates of dry deposition as described by Clarke *et al*. (1997). A comparison of concentration estimates using ADS during the CELTIC study at Duke Forest and filter packs from the Candor CASTNet site suggested a possible bias in the partitioning between $HNO_3$ and $NO_3^-$ (Table 3) in the CASTNet data.

**Table 3** Comparison of Duke Forest ADS measurements and filter pack measurements made at the Candor CASTNet site

| | $NH_4^+$ | $HNO_3$ | $NO_3^-$ | $HNO_3 + NO_3^-$ |
|---|---|---|---|---|
| *Week 28/29* | | | | |
| Duke Forest | 2.25 | 0.51 | 1.08 | 1.59 |
| Candor (unadjusted) | 1.81 | 1.52 | 0.06 | 1.58 |
| Candor (adjusted) | 2.16 | 1.44 | 0.14 | 1.58 |
| *Annual* | | | | |
| Candor (unadjusted) | 1.46 | 1.77 | 0.55 | 2.32 |
| Candor (adjusted) | 1.65 | 1.57 | 0.75 | 2.32 |

$HNO_3$, $NO_3^-$, and total $HNO_3 + NO_3^-$ concentrations ($\mu g\,m^{-3}$) include reported values (unadjusted) and concentrations adjusted using the ISORROPIA gas–aerosol equilibrium model (adjusted). CASTNet, Clean Air Status and Trends Network.

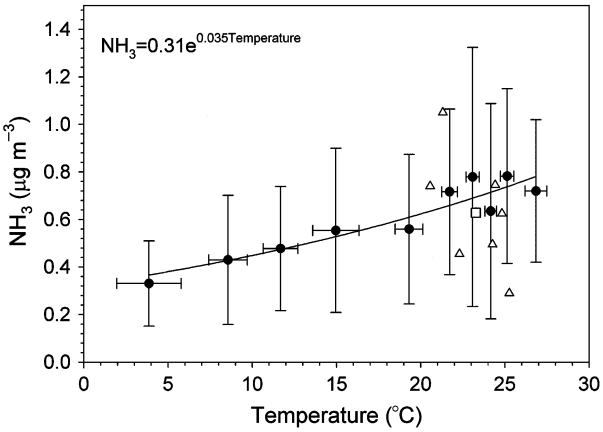


**Fig. 5** Ammonia concentrations vs. air temperature. Black dots represent bin-averaged data ($N = 12$) from a nonagricultural coastal site in eastern North Carolina. Error bars represent $\pm 1$ standard deviation from the mean. Black line represents regression fit to bin-averaged data. Triangles and square represent daily and overall average concentrations, respectively, measured during Chemical Emission, Loss, Transformation and Interactions within Canopies (CELTIC) study.

Revolatilization of $NH_4NO_3$ from the Teflon particulate filter within the CASTNet filter pack system may impart a negative bias to $NO_3^-$ and a corresponding positive bias in the $HNO_3$ (which is more readily deposited) collected, leaving the sum of $HNO_3 + NO_3^-$ unaffected (Table 3; Harrison & Kitto, 1990; Sickles, 1999). Under scenario (2), CASTNet $HNO_3$ concentrations were first adjusted for potential positive bias resulting from $NH_4NO_3$ volatilization on the collection filter using the ISORROPIA gas–aerosol equilibrium model (Nenes *et al*., 1998), estimated $NH_3$ concentrations (Fig. 5; Walker *et al*., 2004), and meteorological data from the CASTNet site. Candor CASTNet deposition velocities derived from the MLM were then applied to these adjusted weekly concentrations to estimate deposition.

Under scenarios (3) and (4), deposition velocities were derived from a single-layer resistance model used during CELTIC with bulk canopy resistances ($R_c$) of 15 and 0 $s\,m^{-1}$, respectively, using Duke Forest meteorology. These deposition velocities were then applied to the adjusted Candor $HNO_3$ concentrations to yield weekly deposition estimates for Duke Forest. In each of the four scenarios, hourly fluxes were calculated by applying weekly average concentrations to hourly deposition velocities.

$HNO_3$ scenarios (1) and (2) yielded annual deposition rates to Duke Forest of 1.56 and 1.38 $kg\,N\,ha^{-1}$, respectively (Table 2), suggesting that correction of CASTNet filter pack measurements for $NH_4NO_3$ loss at the Candor site had a relatively small effect on annual deposition estimates. The average deposition velocity for scenarios (1) and (2) was 1.3 $cm\,s^{-1}$. Scenarios (3) and (4) yielded annual deposition rates of 1.95 and 2.9 $kg\,N\,ha^{-1}$, respectively, which illustrates the importance of estimating the bulk canopy resistance ($R_c$) term accurately. Changes in the canopy resistance ($R_c = 0$–15 $s\,m^{-1}$) can lead to substantial differences in the deposition estimate that will become larger when extrapolated to annual or longer time scales. Average deposition velocities for scenarios (3) and (4) were 1.8 and 2.7 $cm\,s^{-1}$, respectively. Scenario (3) likely produces the most accurate estimate of annual deposition, because this approach is consistent with recent measurements of $R_c > 0$ (Tarnay *et al*., 2002; Nemitz *et al*., 2004) and utilizes Duke Forest meteorology.

Particulate $NO_3^-$ and $NH_4^+$ dry deposition rates were each estimated using the same three scenarios. Scenario (1) used the unadjusted CASTNet deposition from the Candor site as a direct estimate. Similar to the estimate of $HNO_3$ deposition, scenario (2) used concentrations that were first adjusted for the possible bias resulting from $NH_4NO_3$ volatilization on the CASTNet filter pack measurements. CASTNet deposition velocities for the Candor site were then used with the adjusted concentrations to estimate weekly deposition at Duke Forest. Scenario (3) used the same corrected concentration measurements as scenario (2), but deposition velocities were derived from the modified version of Slinn's model (Ruijgrok *et al*., 1997) used during CELTIC with Duke Forest meteorology. These deposition velocities were then applied to the adjusted Candor CASTNet concentrations to estimate weekly deposition at Duke Forest. In each scenario, hourly fluxes were calculated by applying weekly average concentrations to hourly deposition velocities.

Scenarios (1) and (2) yielded particulate $NO_3^-$ annual deposition rates of 0.043 and 0.058 $kg\,N\,ha^{-1}$, respec-

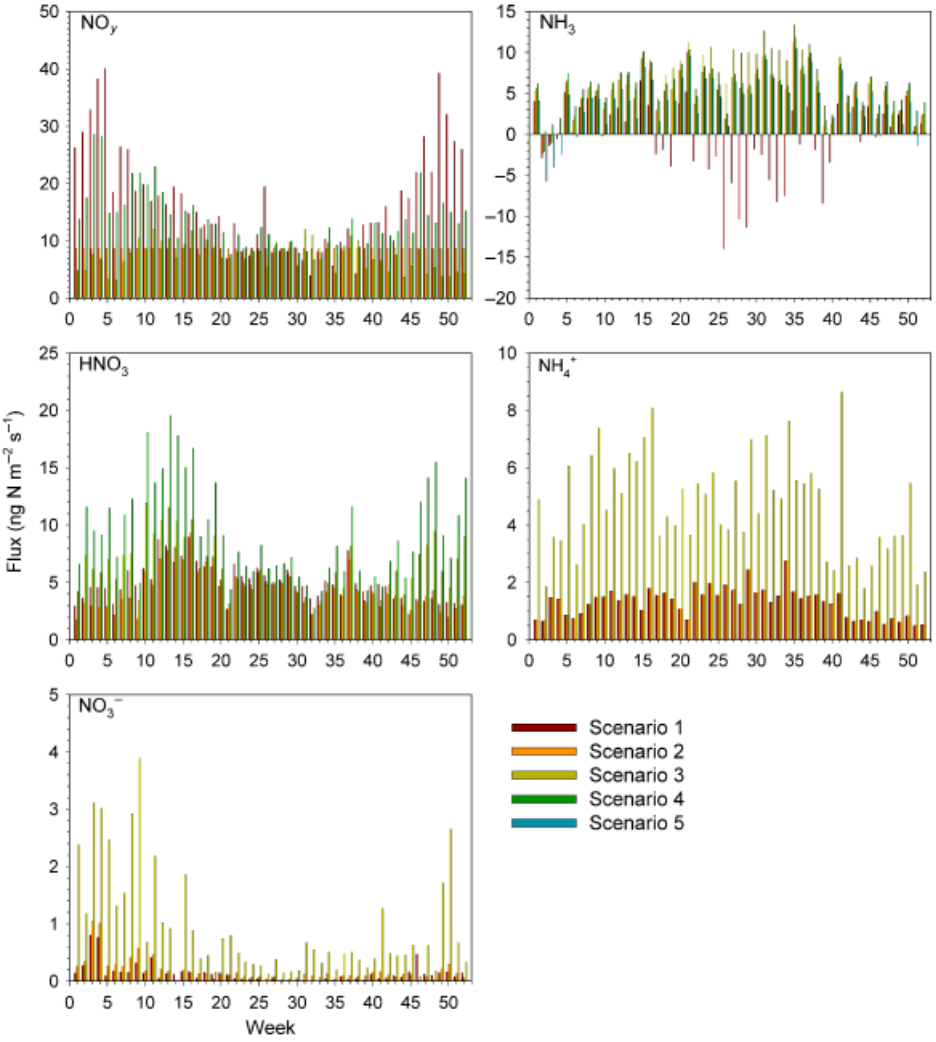


**Fig. 6** Weekly sums of N deposition calculated for 2003 using the different scenarios described in the text for $NO_y$, $HNO_3$, $NH_3$, $NO_3^-$, and $NH_4^+$.

tively (Table 2). Adjusting the filter pack concentration measurements for potential $NH_4NO_3$ bias had a significant influence on the calculated annual flux for this chemical species (an increase of $>30\%$). However, the relatively low deposition velocities estimated using MLM under scenarios (1) and (2) (average $V_d = 0.11\,cm\,s^{-1}$) indicated dry $NO_3^-$ was a relatively small fraction of the total atmospheric N input compared with other chemical species examined in this study. The modified Slinn model used under scenario (3) predicted higher deposition velocities for particulate $NO_3^-$ compared with those predicted by MLM (average $V_d = 0.56\,cm\,s^{-1}$). The deposition velocities predicted by the modified Slinn model are more consistent with measured deposition velocities of particles over tall vegetation (Gallagher *et al*., 1997) and is likely the more robust estimate of true deposition. The annual flux of particulate $NO_3^-$ calculated under scenario (3) was $0.29\,kg\,N\,ha^{-1}$.

The average particulate $NH_4^+$ concentration at the Candor CASTNet site during 2003 [scenario (1)] increased by 13% (Table 3) when adjusted for potential volatilization losses during sampling [scenario (2)]. Annual particulate $NH_4^+$ fluxes calculated under scenarios (1) and (2) (MLM derived average $V_d = 0.11\,cm\,s^{-1}$) were 0.41 and $0.46\,kg\,N\,ha^{-1}$, respectively. Similar to particulate $NO_3^-$, scenario (3) yielded significantly larger deposition velocities than scenarios (1) and (2) (average $V_d = 0.42\,cm\,s^{-1}$) and, subsequently, a higher annual particulate $NH_4^+$ deposition rate of $1.67\,kg\,N\,ha^{-1}$, respectively. Again, due to agreement of the Slinn model with measured values, we recommend this as our best estimate of $NH_4^+$ deposition.

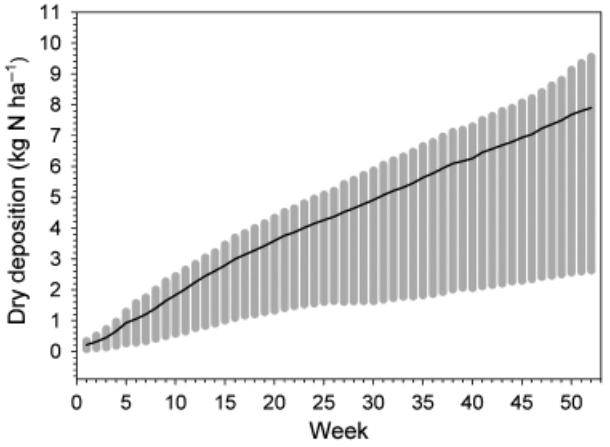


**Fig. 7** Plot of cumulative nitrogen deposition by dry deposition calculated for 2003. The line represents our 'best' estimate with the vertical bars representing the range of all scenarios.

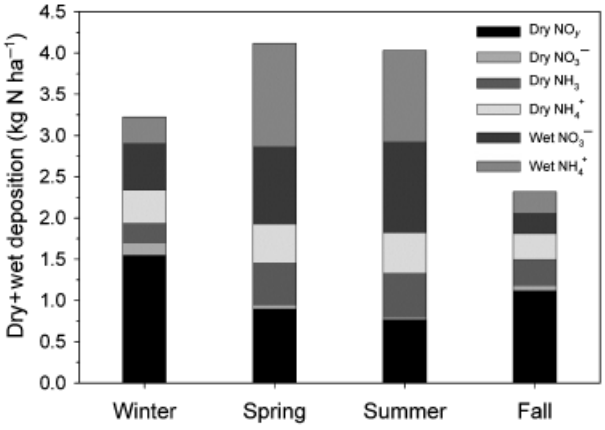


**Fig. 8** Plot of seasonal contribution to nitrogen deposition by wet and dry deposition, as well as components of the dry deposition.

### *Annual $NH_3$ fluxes*

Ammonia fluxes were estimated using five scenarios. First, a time series of hourly $NH_3$ concentrations for 2003 was constructed using the temperature relationship shown in Fig. 5 from an eastern North Carolina nonagricultural site. Ambient concentrations were then used to estimate fluxes using the canopy compensation point model employed during the CELTIC study (described in the previous section). The five modeling scenarios represented a range of soil emissions and leaf (stomatal) emission potentials ($\Gamma_s$): (1) intermediate soil emission (5 ng N m$^{-2}$ s$^{-1}$) and high $\Gamma_s = 1000$; (2) intermediate soil emission and intermediate $\Gamma_s = 250$; (3) intermediate soil emission and low $\Gamma_s = 50$; (4) low soil emission (1 ng N m$^{-2}$ s$^{-1}$) and intermediate $\Gamma_s$; and (5) high soil emission (10 ng N m$^{-2}$ s$^{-1}$) and intermediate $\Gamma_s$. Ranges of $\Gamma_s$ (Flechard & Fowler, 1998; Schjoerring *et al*., 1998; Milford *et al*., 2001) and soil emissions (Walker *et al*., 2002) were based on values previously reported for unfertilized systems.

Over the range of values used in this analysis, $\Gamma_s$ has a larger influence on the annual flux estimate than soil emission rate (Table 2). Under scenario (1) (low $\Gamma_s$), the calculated annual deposition rate was 2.07 kg N ha$^{-1}$, while scenario (3) (high $\Gamma_s$) yielded a net annual emission flux of 0.18 kg N ha$^{-1}$. The lower and upper soil emission rates used for scenarios (4) and (5) yielded a range of annual deposition rates between 1.9 and 1.22 kg N ha$^{-1}$. Given that Duke Forest is an unfertilized plantation forest and there are no available direct measurements, scenario (2) (i.e. intermediate values of $\Gamma_s$ and soil emission) is likely the most reasonable estimate. Scenario (2) produced an annual deposition rate of 1.59 kg N ha$^{-1}$.

### *Annual estimates and seasonal trends*

Figure 6 shows the range of weekly deposition estimates for each chemical species under the scaling scenarios described above. During the winter months, dry deposition under all scenarios is dominated by $NO_y$. Interestingly, under most scenario runs, $HNO_3$ accounts for a relatively small portion of the total $NO_y$ addition (32–67% of $NO_y$). This is important for two reasons. First, it implies strongly that other forms of $NO_y$ (most likely organic peroxy and alkyl nitrate compounds) are a significant portion of the total flux. Second, if organic forms of $NO_y$ are a large portion of the flux, it casts doubt on the completeness of estimates derived from CASTNet and other dry deposition assessments. CASTNet does not measure organic forms of dry deposition. In fact, CASTNet only quantifies $HNO_3$ in the gas phase and may significantly underestimate total dry N deposition in many environments.

In general, modeled fluxes of individual chemical species tended to follow the seasonal pattern of ambient concentration instead of being limited by such things as plant or stomatal activity. $HNO_3$ concentrations were highest during winter and spring, primarily in response to higher $NO_x$ emissions. Particulate $NO_3^-$ concentrations were also highest during the colder months when $HNO_3$ was more abundant and low temperatures shift the equilibrium of $NH_4NO_3$ toward the aerosol phase. Particulate $NH_4^+$ is primarily associated with $SO_4^{-2}$ at this site. Thus, higher concentrations of $NH_4^+$ during spring and summer result from the temperature dependence of $NH_3$ emissions from agricultural and biogenic sources, as well as seasonality in $SO_2$ oxidation rates.

Ammonia deposition was estimated to be highest during the summer when higher ambient concentra-

**Table 4** Wet and dry deposition of nitrogen to Duke Forest during 2003 assuming 'best estimate' scenarios. Wet deposition estimates are averages from the three nearest NADP sites: NC34, NC36, and NC41 (NADP, 2005)

| | Winter ($kg\,N\,ha^{-1}$) | Spring ($kg\,N\,ha^{-1}$) | Summer ($kg\,N\,ha^{-1}$) | Fall ($kg\,N\,ha^{-1}$) | Annual ($kg\,N\,ha^{-1}$) | % of total |
|---|---|---|---|---|---|---|
| *Dry* | | | | | | |
| $NO_y$ | 1.55 | 0.9 | 0.77 | 1.12 | 4.34 | 31.7 |
| $NO_3^-$ | 0.15 | 0.05 | 0.03 | 0.06 | 0.29 | 2.1 |
| $NH_3$ | 0.24 | 0.51 | 0.53 | 0.32 | 1.59 | 11.6 |
| $NH_4^+$ | 0.40 | 0.47 | 0.49 | 0.31 | 1.67 | 12.2 |
| *Wet* | | | | | | |
| $NO_3^-$ | 0.57 | 0.94 | 1.10 | 0.25 | 2.86 | 20.9 |
| $NH_4^+$ | 0.32 | 1.25 | 1.11 | 0.26 | 2.94 | 21.5 |
| *Dry + Wet* | 3.23 | 4.11 | 4.03 | 2.32 | 13.69 | – |

See text for scenario descriptions and selection of particular scenarios for the best estimate calculation.

tions and lower stomatal and cuticular resistances tend to reduce the overall canopy compensation point. Deposition rates were highest at night when stomatal exchange ceases and surface moisture promotes rapid cuticular uptake. Lower deposition rates or periods of emission occur during the day when surfaces are dry and the stomatal compensation point increases in response to temperature. This diurnal pattern is consistent across seasons, indicating that ambient $NH_3$ concentrations are always near the canopy compensation point.

Figure 7 describes the cumulative weekly dry deposition of $NO_y$, $NH_3$, particulate $NO_3^-$, and particulate $NH_4^+$ over the course of 2003. The central line is our best estimate of total deposition arrived at by combining what we felt were the most robust scaling scenarios for each chemical species. The gray area around the best estimate line represents the range of estimates from all scenarios. Using the respective 'best estimate' scenarios for each chemical species, dry deposition of $NO_y$, $NH_3$, $NO_3^-$, and $NH_4^+$ during 2003 totaled approximately $7.90\,kg\,N\,ha^{-1}$. Upper and lower limits on annual dry N deposition were estimated from the combination of scenarios for individual chemical species, which yielded the highest ($9.55\,kg\,N\,ha^{-1}$) and lowest annual deposition rates ($2.63\,kg\,N\,ha^{-1}$). While wet N deposition shows strong seasonality, peaking in spring and summer, the accumulation of N from dry deposition rates early in the year result from higher $NO_2$ concentrations during the winter months.

The combination of our best estimate of dry deposition and measured wet deposition ($NO_3^-$ and $NH_4^+$; no measurement of organic N) resulted in an N deposition to Duke Forest of $13.7\,kg\,N\,ha^{-1}$ during 2003 (Fig. 8, Table 4). The seasonal variability of total deposition was primarily driven by the wet fraction with the highest wet deposition of $NO_3^-$ and $NH_4^+$ occurring during the spring and summer. On an annual basis, dry deposition accounted for approximately 58% of total N deposition (Table 4).

The results presented here have three important implications. First, it shows that reasonably constrained estimates of dry N deposition can be generated for sites of ecological interest such as a FACE site using short-term flux measurements and regional concentration estimates. Second, the monitoring of gaseous $HNO_3$ and particulate nitrate and ammonia as is done across the CASTNet network potentially significantly underestimates total dry N deposition. Third, significant dry deposition of N occurs during the winter and monitoring only during the growing season captures only a portion of the annual flux. These observations taken together strongly suggest that current strategies for estimating dry deposition of N potentially suffer from significant limitations.

Recent modeling efforts (Ollinger *et al*., 2002; Thornton *et al*., 2002) have suggested exogenous N inputs will likely have significant implications for future forest production, growth, and, ultimately, carbon sequestration. Our results suggest that modeling based upon parameterizations from national deposition networks (e.g. NADP and CASTNet) only may significantly underestimate dry N deposition. Therefore, a priority should be placed on generating robust estimates of dry N deposition including organic forms and ammonia.

## Acknowledgements

Funding for this study was provided by the National Science Foundation (NSF), Award # DEB-0237674 to Jed Sparks. We thank Dave Whitall (NOAA) and Hans Paerl (UNCIMS) for denuder data collected at the UNC Institute of Marine Sciences in Morehead City, NC. We also thank Wayne Robarge (NCSU) for analysis of denuder/filter pack samples collected during CELTIC and Mark Barnes (NCSU) for deploying the denuder systems. We thank Wayne Cornelius of the North Carolina Division of Air Quality for assistance with trace gas monitoring

 

data. We would like to thank the Duke FACE site and its staff for allowing us to work at their research site as well as the invaluable assistance they provided during the CELTIC experiment. We would also like to thank Gabriel Katul for access to Duke Forest meteorological data. The Duke FACE site is supported by the Office of Science (BER), US Department of Energy, Grant No. DE-FG02–95ER62083. The US Environmental Protection Agency, through its Office of Research and Development, collaborated in the research described here. This publication has been subjected to the Agency's peer and administrative review and has been approved for publication as an EPA document. Mention of trade names or commercial products does not constitute endorsement by EPA.

## References

Bazzaz FA, Miao SL (1993) Successional status, seed size, and response of tree seedlings to $CO_2$, light and nutrients. *Ecology*, **74**, 104–112.

Brook JR, Zhang L, Di-Giovanni F, Padro J (1999) Description and evaluation of a model of deposition velocities for routine estimates of air pollutant dry deposition over North America. Part I: model development. *Atmospheric Environment*, **33**, 5037–5051.

CASTNet (2005) *Clean Air Status and Trends Network*. http://www.epa.gov/castnet/index.html

Clarke JF, Edgerton ES, Martin BE (1997) Dry deposition calculations for the clean air status and trends network. *Atmospheric Environment*, **31**, 3667–3678.

Curtis PS, Wang XZ (1998) A meta-analysis of elevated $CO_2$ effects on woody plant mass, form, and physiology. *Oecologia*, **113**, 299–313.

De Miguel A, Bilbao J (1999) Ozone dry deposition and resistances onto green grassland in summer in central Spain. *Journal of Atmospheric Chemistry*, **34**, 321–338.

Dollard GJ, Atkins DHF, Davies TJ, Healy C (1987) Concentrations and dry deposition velocities of nitric acid. *Nature*, **326**, 481–483.

Duyzer JH, Deinum G, Baak J (1995) The interpretation of measurements of surface exchange of nitrogen-oxides – correction for chemical reactions. *Philosophical Transactions of the Royal Society of London*, **351**, 231–248.

Duyzer JH, Dorsey JH, Gallagher MW, Walton S (2004) Oxidised nitrogen and ozone interaction wit forests 2: multi-layer process oriented modeling results and sensitivity study for Douglas Fir. *Quarterly Journal of the Royal Meteorological Society*, **130**, 1957–1971.

Duyzer JH, Verhagen HLM, Westrate JH (1992) Measurement of the dry deposition flux of $NH_3$ on to coniferous forest. *Environmental Pollution*, **75**, 3–13.

Fahey DW, Eubank CS, Hubler G, Fehsenfeld FC (1985) Evaluation of a catalytic reduction technique for the measurement of total reactive odd-nitrogen $NO_y$ in the atmosphere. *Journal of Atmospheric Chemistry*, **3**, 435–468.

Farmer DK, Wooldridge PJ, Cohen RC (2006) Application of thermal-dissociation laser induced fluorescence (TD-LIF) to measurement of $HNO_3$, $\sum$ alkyl nitrates, $\sum$ peroxy nitrates, and $NO_2$ fluxes using eddy covariance. *Atmospheric Chemistry and Physics Discussion*, **6**, 1–42.

Flechard CR, Fowler D (1998) Atmospheric ammonia at a moorland site. II: longterm surface-atmospheric micrometeorological flux measurements. *Quarterly Journal of the Royal Meteorological Society*, **124**, 759–791.

Gallagher MW, Beswick KM, Duyzer J, Westrate H, Choularton TW, Hummelshoj P (1997) Measurements of aerosol fluxes to Speulder forest using a micrometeorological technique. *Atmospheric Environment*, **31**, 359–373.

Garland JA (1977) The dry deposition of $SO_2$ on agricultural crops. *Atmospheric Environment*, **12**, 369–373.

Gessler A, Rienks M, Rennenberg H (2000) $NH_3$ and $NO_2$ fluxes between beech trees and the atmosphere – correlation with climatic and physiological parameters. *New Phytologist*, **147**, 539–560.

Hamilton JG, DeLucia EH, George K, Naidu SL, Finzi AC, Schlesinger WH (2002) Forest carbon balance under elevated $CO_2$. *Oecologia*, **131**, 250–260.

Hanson PJ, Rott K, Taylor GE, Gunderson CA, Lindberg SE, Rosstodd BM (1989) $NO_2$ deposition to elements representative of a forest landscape. *Atmospheric Environment*, **23**, 1783–1794.

Harrison RM, Kitto AM (1990) Field intercomparison of filter pack and denuder sampling methods for reactive gaseous and particulate pollutants. *Atmospheric Environment*, **24A**, 2633–2640.

Hereid DP, Monson RK (2001) Nitrogen oxide fluxes between corn (*Zea mays* L.) leaves and the atmosphere. *Atmospheric Environment*, **35**, 975–983.

Horii CV, Munger JW, Wofsy SC, Zahniser M, Nelson D, McManus JB (2005) Atmospheric reactive nitrogen concentration and flux budgets at a Northeastern US forest site. *Agricultural and Forest Meteorology*, **133**, 210–225.

Hicks BB, Baldocchi DD, Meyers TP, Hosker RP, Matt DR (1987) A preliminary multiple resistance routine for describing dry deposition velocities from measured quantities. *Water Air and Soil Pollution*, **36**, 311–330.

Kaimal JC, Finnigan JJ (1994) *Atmospheric Boundary Layer Flows: Their Structure and Measurement*. Oxford University Press, Oxford, pp. 124–154.

Katul GG, Albertson JD (1999) Modeling $CO_2$ sources, sinks, and fluxes within a forest canopy. *Journal of Geophysical Research – Atmospheres*, **104**, 6081–6091.

Lovett GM, Traynor MM, Pouyat RV, Carreiro MM, Zhu WX, Baxter JW (2000) Atmospheric deposition to oak forests along an urban–rural gradient. *Environmental Science and Technology*, **34**, 4294–4300.

Luo YQ, Reynolds J, Wang YP, Wolfe D (1999) A search for predictive understanding of plant responses to elevated [$CO_2$]. *Global Change Biology*, **5**, 143–156.

Meetham AR (1950) Natural removal of pollution from the atmosphere. *Quarterly Journal of the Royal Meteorological Society*, **76**, 359–364.

Meyers TP, Finkelstein PL, Clarke J, Ellestad TG, Sims P (1998) A multilayer model for inferring dry deposition using standard meteorological measurements. *Journal of Geophysical Research*, **103**, 22645–22661.

Meyers TP, Hall ME, Lindberg SE, Kim K (1996) Use of the modified Bowen-ratio technique to measure fluxes of trace gases. *Atmospheric Environment*, **30**, 3321–3329.

 

Meyers TP, Huebert BJ, Hicks BB (1989) $HNO_3$ deposition to a deciduous forest. *Boundary-Layer Meteorology*, **49**, 395–410.

Milford C, Hargreaves KJ, Sutton MA, Loubet B, Cellier P (2001) Fluxes of $NH_3$ and $CO_2$ over upland moorland in the vicinity of agricultural land. *Journal of Geophysical Research*, **106**, 24169–24181.

Monteith JL, Unsworth M (1990) *Principles of Environmental Physics*, 2nd edn. Arnold Press, London.

Munger JW, Wofsy SC, Bakwin PS *et al*. (1996) Atmospheric deposition of reactive nitrogen oxides and ozone in a temperate deciduous forest and subarctic woodland 1. Measurements and mechanisms. *Journal of Geophysical Research*, **101**, 12639–12657.

NADP (2005) *National Atmospheric Deposition Program (NRSP-3)*. NADP Program Office, Illinois State Water Survey, Champaign, IL. http://nadp.sws.uiuc.edu

NC DAQ (2005) *North Carolina Division of Air Quality*. http://daq.state.nc.us/

Nemitz E, Milford C, Sutton MA (2001) A two-layer canopy compensation point model for describing bi-directional biosphere–atmosphere exchange of ammonia. *Quarterly Journal of the Royal Meteorological Society*, **127**, 815–833.

Nemitz E, Sutton MA, Schjoerring JK, Husted S, Wyers GP (2000) Resistance modeling of ammonia exchange over oilseed rape. *Agricultural and Forest Meteorology*, **105**, 405–425.

Nemitz E, Sutton MA, Wyers GP, Jongejan PAC (2004) Gas–particle interactions above a Dutch heathland: 1. Surface exchange fluxes of $NH_3$, $SO_2$, $HNO_3$, and HCl. *Atmospheric Physics and Chemistry*, **4**, 989–1005.

Nenes A, Pandis SN, Pilinis C (1998) ISORROPIA: a new thermodynamic equilibrium model for multiphase multicomponent inorganic aerosols. *Aquatic Geochemistry*, **4**, 123–152.

Ollinger SV, Aber JD, Reich PB, Freuder R (2002) Interactive effects of nitrogen deposition, tropospheric ozone, elevated $CO_2$ and land use history on the carbon dynamics of northern hardwood forests. *Global Change Biology*, **8**, 545–562.

Oren R, Ellsworth DS, Johnsen KH *et al*. (2001) Soil fertility limits carbon sequestration by forest ecosystems in a $CO_2$-enriched atmosphere. *Nature*, **411**, 469–472.

Pan YD, Melillo JM, McGuire AD *et al*. (1998) Modeled responses of terrestrial ecosystems to elevated atmospheric $CO_2$: a comparison of simulations by the biogeochemistry models of the vegetation/ecosystem modeling and analysis project (VEMAP). *Oecologia*, **114**, 389–404.

Pryor SC, Barthelmie RJ, Sorenson LL, Jensen B (2001) Ammonia concentrations and fluxes over a forest in the midwestern USA. *Atmospheric Environment*, **35**, 5645–5656.

Ruijgrok W, Tieben H, Eisinga P (1997) The dry deposition of particles to a forest canopy: a comparison of model and experimental results. *Atmospheric Environment*, **31**, 399–415.

Schimel DS, House JI, Hibbard KA *et al*. (2001) Recent patterns and mechanisms of carbon exchange by terrestrial ecosystems. *Nature*, **414**, 169–172.

Schjoerring JK, Husted S, Mattsson M (1998) Physiological parameters controlling plant-atmosphere ammonia exchange. *Atmospheric Environment*, **32**, 491–498.

Sickles JE (1999) A summary of airborne concentrations of sulfur- and nitrogen-containing pollutants in the northeastern Unites States. *Journal of Air Waste Management Association*, **49**, 882–893.

Slinn WGN (1982) Predictions for particle deposition to vegetative canopies. *Atmospheric Environment*, **16**, 1785–1794.

Sparks JP, Monson RK, Sparks KL, Lerdau M (2001) Leaf uptake of nitrogen dioxide ($NO_2$) in a tropical wet forest: implications for troposheric chemistry. *Oecologia*, **127**, 214–221.

Sparks JP, Roberts JM, Monson RK (2003) The uptake of gaseous organic nitrogen by leaves: a significant global nitrogen transfer process. *Geophysical Research Letters*, **30**, 2189.

Sutton MA, Burkhardt JK, Guerin D, Nemitz E, Fowler D (1998) Development of resistance models to describe measurements of bi-directional ammonia surface–atmosphere exchange. *Atmospheric Environment*, **32**, 473–480.

Sutton MA, Place CJ, Eager M, Fowler D, Smith RI (1995) Assessment of the magnitude of ammonia emissions in the United Kingdom. *Atmospheric Environment*, **29**, 1393–1411.

Tarnay LW, Gertler A, Taylor GW (2002) The use of inferential models for estimating nitric acid vapor deposition to semi-arid coniferous forests. *Atmospheric Environment*, **36**, 3277–3287.

Thornton PE, Law BE, Gholz HL *et al*. (2002) Modeling and measuring the effects of disturbance history and climate on carbon and water budgets in evergreen needleleaf forests. *Agricultural and Forest Meteorology*, **113**, 185–222.

Turnipseed AA, Huey LG, Nemitz E *et al*. (2006) Eddy covariance fluxes of Peroxyacyl nitrates (PANs) and $NO_y$ to a coniferous forest. *Journal of Geophysical Research – Atmospheres*, **111**, 6214–6224.

US EPA (1997) Determination of reactive acidic and basic gases and strong acidity of fine particles ($<2.5$ m). In: *Compendium of Methods for the Determination of Inorganic Compounds in Ambient Air, Method IO-42. EPA-625/R-96/010a*. Center for Environmental Research Information, Office of Research and Development, Cincinnati, OH.

US EPA (2004) *Clean Air Status and Trends Network (CASTNet) 2003 Annual Report*. Office of Air and Radiation, Research Triangle Park, NC.

Walker JT, Geron C, Vose J, Swank W (2002) Nitrogen trace gas emissions from a riparian ecosystem in Southern Appalachia. *Chemosphere*, **49**, 1389–1398.

Walker JT, Whitall D, Robarge WP, Paerl H (2004) Ambient ammonia and ammonium aerosol across a region of variable ammonia emission density. *Atmospheric Environment*, **38**, 1235–1246.

Williams EJ, Baumann K, Roberts JM *et al*. (1998) Intercomparison of ground-based $NO_y$ measurement techniques. *Journal Geophysical Research*, **103**, 22261–22280.

Williams EJ, Roberts JM, Baumann K, Bertman SB, Buhr S, Norton RB, Fehsenfeld FC (1997) Variations in $NO_y$ composition at Idaho Hill, Colorado. *Journal Geophysical Research*, **102**, 6297–6314.

Wyers GP, Erisman JW (1998) Ammonia exchange over coniferous forest. *Atmospheric Environment*, **32**, 441–451.

Zak DR, Pregitzer KS, Curtis PS, Vogel CS, Holmes WE, Lussenhop J (2000) Atmospheric $CO_2$, soil-N availability, and allocation of biomass and nitrogen by *Populus tremuloides*. *Ecological Applications*, **10**, 34–46.

 